Dynamical organization around turbulent bursts

Fridolin Okkels* and Mogens H. Jensen†
Niels Bohr Institute and Center for Chaos and Turbulence Studies, Blegdamsvej 17, DK-2100 Ø, Denmark
(Received 6 October 1997)

The detailed dynamics around intermittency bursts is investigated in turbulent shell models. We observe that the amplitude of the high wave number velocity modes vanishes before each burst, meaning that the fixed point in zero and not the Kolmogorov fixed point determines the intermittency. The phases of the field organize during the burst, and after a burst the field oscillates back to the laminar level. We explain this behavior from the variations in the values of the dissipation and the advection around the zero fixed point. [S1063-651X(98)03306-6]

PACS number(s): 47.27.Jv, 05.45.+b, 64.60.Lx

One of the most fundamental problems in turbulence research is the understanding of intermittency effects [1]. In fully developed turbulent flows laminar quiescent periods are interrupted by strong intermittency bursts of high energy dissipation. It is well known both from a number of experiments and numerical simulations that intermittency effects cause corrections to the classical Kolmogorov theory [2] when the structure functions of the velocity field are statistically averaged over space and/or time [1]. On the other hand very little is known about the particular structure of intermittency, as, for instance, the shape of and the behavior around a specific intermittent burst. It is the purpose of this paper to present a detailed investigation of the behavior of the velocity field before and after a burst takes place. We observe a consistent picture in which the velocity gradients, over a small scale, always becomes organized and vanish just before the energy burst sets in by an ''explosion'' in the field. This is like a ''calm before the storm'' and one can draw an analogy to depinning charge-density waves, which phase organize just before they slip [3], or self-organized-critical systems in general where bursts or ''avalanches'' of all sizes can be triggered even by the slightest perturbation [4]. We draw our conclusions from investigations of shell models for turbulence, which are completely deterministic systems where the intriguing structure of intermittency is created by the internal chaotic dynamics. Our results indicate that the trivial fixed point in zero and not the Kolmogorov fixed point [5,6] is responsible for the intermittency. Shell models are formed by various truncation techniques of the Navier-Stokes equations and have become paradigm models for the study of turbulence at very high Reynolds numbers [5]. The mostly studied shell model is the model of Gledzer-Ohkitani-Yamada (GOY) [6–14]. This model yields corrections to the Kolmogorov theory [9] in good agreement with experiments [15–17].

For the GOY shell model, the wave-number space is divided into N separated shells each characterized by a wave-number $k_n=\lambda^n k_0$ $(\lambda=2)$, with $n=1,\ldots,N$. The corresponding amplitude of the velocity field at shell n is a complex variable u_n. By assuming interactions among nearest and next nearest neighbor shells and phase space volume conservation one arrives at the following evolution equations [8]:

$$\left(\frac{d}{dt}+\nu k_n^2\right)u_n = ik_n\left(a_n u_{n+1}^* u_{n+2}^* + \frac{b_n}{2}u_{n-1}^* u_{n+1}^* + \frac{c_n}{4}u_{n-1}^* u_{n-2}^*\right) + f\delta_{n,4}, \tag{1}$$

with boundary conditions $b_1=b_N=c_1=c_2=a_{N-1}=a_N=0$. f is an external, constant forcing, here on the fourth mode.

The coefficients of the nonlinear terms must follow the relation $a_n+b_{n+1}+c_{n+2}=0$ in order to satisfy the conservation of energy, $E=\Sigma_n|u_n|^2$, when $f=\nu=0$. The constraints still leave a free parameter δ so that one can set $a_n=1$, $b_n=-\delta$, $c_n=-(1-\delta)$ [13]. If helicity conservation is also demanded, one obtains the canonical value $\delta=1/2$ [12]. The set (1) of N coupled ordinary differential equations can be numerically integrated by standard techniques. In the simulations, we use the following values: $\delta=1/2$, $N=19$, $\nu=10^{-6}$, $k_0=2^{-5}$, $f=(1+i)0.005$.

Taking a closer look at the dynamics of the GOY model in terms of the complex field $u_n(t)=r_n(t)\,e^{i\theta_n(t)}$, the intermittent bursts consist of a collection of different organizations of the amplitudes r_n, which travel with exponentially increasing speed from the lower up towards the higher shells, where they are damped away by viscosity [18]. Every burst in the model follows a common pattern, where the most prominent characteristic is that the amplitudes of the higher modes vanish just before a burst, as shown in Fig. 1. During the attraction towards $u_n=0$ the phases θ_n organize in period three in the shell index n. Just at the point of minimum amplitude, the phases change so that a new organization of period three occurs during the rapid repulsion from zero. After the burst the modes oscillate back to the laminar level with increasing oscillation periods (Fig. 1).

In order to explain these findings we will use that the period 3 organization of the phases is present not only at bursts, but also during most of the evolution. To argue for this, Fig. 2 shows a long time average of the phase differences $P_n(t)=|\theta_n-\theta_{n-3}|$. We observe, that the assumption holds very well for the highest shells, i.e., that $\theta_{n-1}=\theta_{n+2}$, $\theta_{n-2}=\theta_{n+1}$ [19]. With this assumption, the GOY model can

*Electronic address: okkels@nbi.dk
†Electronic address: mhjensen@nbi.dk

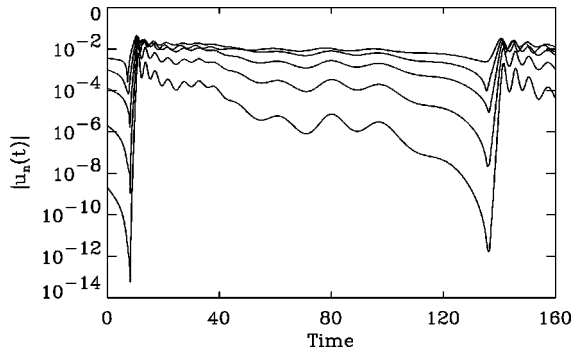

FIG. 1. The temporal evolution [Eq. (1)] of the logarithmic of the modulus of modes corresponding to the highest shells $(r_{15},\ldots,r_{19})$ for a time span between two bursts. The uppermost curve corresponds to shell 15, and the lowest to shell 19. The parameters for the numerical integration are listed in the text.

be separated into two coupled ODE's controlling the evolution of the moduli $r_n(t)$ and the phases $\theta_n(t)$:

$$\dot{r}_n + i r_n \dot{\theta}_n = -\nu k_n^2 r_n + i k_n e^{-iS_n} \times (r_{n+1} r_{n+2} - \tfrac{1}{4} r_{n-1} r_{n+1} - \tfrac{1}{8} r_{n-2} r_{n-1}). \tag{2}$$

Both sides have been multiplied by $e^{-i\theta_n}$ and we have introduced the new variable $S_n(t) = \Sigma_{j=0}^{2} \theta_{n+j}(t)$, $n = 1,\ldots,N-2$ with the boundary conditions $S_{N-2}(t) = S_{N-1}(t) = S_N(t)$. S_n is the natural phase parameter because the evolution of the model is invariant under any rearrangement of the phases in which the values of S_n are conserved [12,19,20]. By separating Eq. (2) into real and imaginary parts, one obtains

$$\dot{r}_n = -\nu k_n^2 r_n + \sin(S_n) R_n, \tag{3}$$

$$\dot{\theta}_n = \cos(S_n) R_n / r_n, \tag{4}$$

where

$$R_n = k_n (r_{n+1} r_{n+2} - \tfrac{1}{4} r_{n-1} r_{n+1} - \tfrac{1}{8} r_{n-2} r_{n-1}). \tag{5}$$

R_n is the real valued coupling from the nearest shells on the nth shell. Combining Eqs. (3) and (4) one eliminates the coupling from the nearest shell and obtains an equation for the time derivative of the phases:

$$\dot{\theta}_n = \cot(S_n) \left(\frac{\dot{r}_n}{r_n} + \nu k_n^2 \right). \tag{6}$$

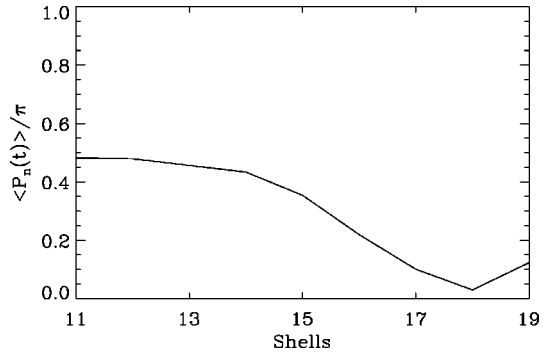

FIG. 2. The time average of $P_n(t) = |\theta_n - \theta_{n-3}|$ normalized by π vs the shell number n. Note that the phase organization corresponding to $P_n(t) \simeq 0$ holds very well for the highest shells. The rise of the graph at $n = 19$ is due to a boundary effect.

If we ignore the two neighboring phases in Eq. (6) and replace S_n with θ_n, simple linear stability analysis of Eq. (6) gives that the phases are attracted/repelled from the fixed points $\theta_n = \pm(\pi/2)$ depending on whether $[(\dot{r}_n/r_n) + \nu k_n^2]$ is negative/positive. Nearly the same stability conditions are found for S_n when the effect of the neighboring phases has been included in Eq. (6) [19]. Direct measurements of the stability of the phases show excellent agreement with the stability predicted by the sign of $[(\dot{r}_n/r_n) + \nu k_n^2]$. The only coupling from the phases on the equation of the moduli [Eq. (3)] is the factor $\sin(S_n)$, which is close to -1 during most of the evolution. If we set $\sin(S_n)$ equal to -1, the effect of the phases is removed from the equation of the moduli, which then becomes a GOY model in terms of real variables. By comparing the evolution of the complex and the real valued GOY model we get an estimate of the effect of the phases on the evolution of the complex GOY model. It turns out that the phases have roughly no effect on the appearance of bursts since the real valued model creates approximately the same bursts as the complex model. We therefore begin by studying the bursts of the real valued model. The main feature of bursts is the attraction and repulsion of the amplitudes to $r_n = 0$, which is a trivial but important fixed point for the model. This dynamics appears as a result of a balance between the viscosity term and the coupling term. In the simplest form the real valued GOY model can be written as

$$\dot{r}_n = V_n + C_n, \tag{7}$$

where $V_n = -\nu k_n^2 r_n$ is the viscosity term and $C_n = -k_n (r_{n+1} r_{n+2} - \tfrac{1}{4} r_{n-1} r_{n+1} - \tfrac{1}{8} r_{n-2} r_{n-1})$ is the coupling term, and where the forcing is neglected because we focus on the dynamics of the high wave numbers. As V_n and r_n are proportional with opposite signs, Eq. (7) can also be written as $\dot{V}_n = -\nu k_n^2 (V_n + C_n)$. The values of $\dot{V}_n$ are shown in Fig. 3 by a grid of arrows. Only the $\dot{V}_n$ field is shown by arrows as this determines the change in the attraction (or repulsion) to (or from) the fixed point. Furthermore, the values of $\dot{C}_n$ are not universal. Also shown are trajectories of (V_n, C_n) during a burst, both of the real valued model (solid) and the complex model (dotted) (for the complex model the moduli are drawn). The dashed straight line shows where the flow vanishes $(\dot{r}_n = 0)$. First we notice that the qualitative similarity between bursts in the real valued and complex model show the weak effect of the phases on bursts. From the flow field in Fig. 3 we see that without variations in the coupling term, the amplitude will stabilize at the dashed line.

Each stage of the dynamics is labeled in Fig. 3. During the attraction, labeled A, the viscosity term and the coupling term balance each other with a slight dominance of the viscosity term. Because the trajectory approaches the fixed point $r_n = 0$ with decreasing velocity and because $|V_n|$ and $|C_n|$ are much larger than $|\dot{r}_n|$, *the trajectory always ap-*

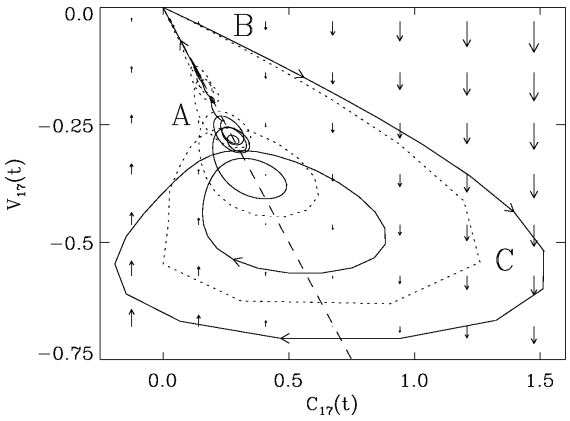

FIG. 3. Trajectories of V_n vs C_n during a burst for the real valued model, Eq. (7) with forcing added (solid curve), and the complex model, Eq. (1) (dotted curve). On the same graph is shown the flow field of the viscosity V_n visualized by arrows. The dashed line shows where $\dot{V}_n=0$. The labels represent the attraction to the fixed point $r_n=0$ (A), the repulsion away from the fixed point (B), and maximum amplitude of the field (C). The arrows on the trajectories indicate the direction of the temporal evolution.

proaches $r_n=0$ tangentially to, but slightly below, the diagonal $V_n=-C_n$. When approaching $r_n=0$ the trajectory can only be kicked away by variations in the coupling term, and the absence of these variations makes the amplitude stabilize close to zero. The delicate balance between V_n and C_n is therefore responsible for the long lasting laminar regimes between the bursts.

As soon as a burst approaches from the lower shells the coupling term becomes large and the trajectory is forced away from $r_n=0$ in a given direction (labeled B in Fig. 3) into a regime of positive $\dot{r}_n$. This direction is not universal; by construction it depends on the value of the amplitudes in the neighboring shells [21]. At the end of the repulsion, labeled C, the coupling becomes less dominant over the viscosity, and this is seen in Fig. 3 as a turning towards the dashed equilibrium line. As this line is crossed, the amplitude reaches its maximum, after which it is again attracted towards zero by the dominance of the viscosity. The motion is highly excited by the burst and the amplitude oscillates around the line. The oscillations are damped away and the amplitude settles again close to the dashed line where the picture is now repeated again beginning at A.

From the above scenario it is possible to give an explanation as to why bursts are created in the GOY model: the amplitude gets trapped at the fixed point in zero and can only be released when a burst arrives from the lower shells. As soon as a weak burst is created at the low shells, it continues all the way to the highest shells because the stability of higher shells are changed by the approaching burst. *The intermittency is created by a ''domino'' effect through the shells.* The highest and the lowest shells evolve differently because the effect of the viscosity reduces towards the low shells. This reduces the attraction of the amplitudes towards zero, which makes it less possible for bursts to occur and gives instead a slow random walk dynamics with Gaussian statistics. The low shells therefore produce slow random perturbations that propagate up through the shells and release bursts at large shells (small scale).

In conclusion, we have described the mechanism of the creation of intermittent bursts in the GOY model. The results show that the creation of a burst is determined by a delicate balance between the viscosity and advection terms. We therefore believe that a similar scenario might be present in other intermittent, turbulent systems and also in experiments. Our main observation is that a burst is associated with a ''fingerprint:'' The amplitudes of the high wave-number modes vanish before the burst. An experimental time signal, say from hot wire measurements, might indeed show similar characteristics. We are in the process of investigating this using wavelet analysis around the bursts. Similar work in this direction has also been done recently by Camussi and Guj [22].

We are grateful to P. Bak, T. Bohr, S. Ciliberto, T. Dombre, K. Hansen, J. Kockelkoren, and G. Zocchi for discussions and suggestions.

[1] U. Frisch, *Turbulence: The Legacy of A.N. Kolmogorov* (Cambridge University Press, Cambridge, 1995).
[2] A.N. Kolmogorov, C. R. Acad. Sci. USSR **30**, 301 (1941); **32**, 16 (1941).
[3] C. Tang, K. Wiesenfeld, P. Bak, S. Coppersmith, and P. Littlewood, Phys. Rev. Lett. **58**, 1161 (1987).
[4] P. Bak, C. Tang, and K. Wiesenfeld, Phys. Rev. Lett. **59**, 381 (1987).
[5] T. Bohr, M. H. Jensen, G. Paladin, and A. Vulpiani, *Dynamical Systems Approach to Turbulence* (Cambridge University Press, Cambridge, in press).
[6] L. Kadanoff, D. Lohse, and N. Schörghofer, Physica D **100**, 165 (1997).
[7] E. B. Gledzer, Sov. Phys. Dokl. **18**, 216 (1973).
[8] M. Yamada and K. Ohkitani, J. Phys. Soc. Jpn. **56**, 4210 (1987); Prog. Theor. Phys. **79**, 1265 (1988).
[9] M. H. Jensen, G. Paladin, and A. Vulpiani, Phys. Rev. A **43**, 798 (1991).
[10] R. Benzi, L. Biferale, and G. Parisi, Physica D **65**, 163 (1993).
[11] D. Pisarenko, L. Biferale, D. Courvasier, U. Frisch, and M. Vergassola, Phys. Fluids A **65**, 2533 (1993).
[12] L. Kadanoff, D. Lohse, J. Wang, and R. Benzi, Phys. Fluids **7**, 617 (1995).
[13] L. Biferale, A. Lambert, R. Lima, and G. Paladin, Physica D **80**, 105 (1995).
[14] N. Schörghofer, L. Kadanoff, and D. Lohse, Physica D **88**, 40 (1995).
[15] F. Anselmet, Y. Gagne, E.J. Hopfinger, and R.A. Antonia, J. Fluid Mech. **140**, 63 (1984).
[16] C. Meneveau and K.R. Sreenivasan, Nucl. Phys. B, Proc. Suppl. **2**, 49 (1987).
[17] J. Herweijer and W. van de Water, Phys. Rev. Lett. **74**, 4651 (1995).
[18] T. Dombre and J.-L. Gilson, Physica D **111**, 265 (1998).
[19] F. Okkels, Master thesis, CATS, University of Copenhagen, Denmark, 1997.

[20] O. Gat, I. Procaccia, and R. Zeitak, Phys. Rev. E **51**, 1148 (1995).

[21] We note that the picture and analysis based on Eq. (7) is local in the sense that only the dynamics of shell n is considered even though the coupling term C_n incorporates the values of amplitudes in the four neighboring shells. A complete picture of the dynamics around the fixed point $r_n=0$, $n=1,\ldots,N$, can be obtained from the center-manifold relating the shells with high viscosity (high n) to the shells with basically no viscosity (marginal modes corresponding to low n). This more mathematical treatment will be presented by the authors in a forthcoming publication. We are grateful to Tomas Bohr for pointing this structure out.

[22] R. Camussi and G. Guj, J. Fluid Mech. **348**, 177 (1998).